Magnetic cellular automata (MCA) systems

M.C.B. Parish and M. Forshaw

Abstract: Single-domain nanomagnets could potentially be used as magnetic logic elements. In this paper, the performance of magnetic cellular automaton (MCA) systems is assessed. The three main types are described briefly and one is analysed in detail. A micromagnetic model which uses Monte Carlo/Metropolis updating is described and shown to be able to reproduce room temperature experimental results. It is subsequently used to investigate a range of MCA system parameters. Emphasis is placed on the potential behaviour of real systems (those which operate at room temperature and which possess fabrication defects). It is found that real adiabatically clocked magnetic systems are likely to operate significantly more slowly than the previously projected limits.

1 Introduction

Since the discovery of giant magnetoresistance (GMR), micromagnetic and nanomagnetic systems have received increasing attention. The majority of this research has been into data storage; for example, patterned recording media, GMR read heads and magnetic random access memory (MRAM) [1]. Recently, several magnetic logic systems have also been proposed [2–5]. They use cellular computation [6, 7] and can be described collectively as magnetic cellular automata (MCA). The three main MCA systems are illustrated in Fig. 1.

The first MCA was the magnetic quantum cellular automaton (MQCA), described by Cowburn and Welland in 2000 [2]. As illustrated in Fig. 1*a*, each active element in the system was a circular disc formed from 10 nm thick supermalloy, with a diameter of 110 nm. These dimensions were small enough to prevent intra-element domain walls forming [8] and each device behaved like a single giant magnetic spin. Each moment was confined to the plane of the element and in an isolated device its ground state direction was infinitely degenerate. To enable the direct encoding of digital information, a bistable (or binary) system is required. Bistability was generated in the MQCA system through interelement interactions. The direction of the moments was collinear with the axis of the chain. The arrow to the right of the chain illustrates the direction in which the external, magnetic 'clock' field was applied. Cowburn and Welland successfully demonstrated the propagation of signals along a magnetic 'wire', by using the clock field to drive a soliton (the interface between two elements with opposing magnetic moments) along the chain of elements.

Cowburn and Welland's experiment was significant because it demonstrated the successful, room temperature, operation of a system of 70 nanoscale magnetic quantum cellular devices. The only other nanoscale cellular automata systems that have been fabricated — electronic quantum cellular automata (EQCA) — currently contain only a small number of elements and operate only at cryogenic temperatures [9, 10].

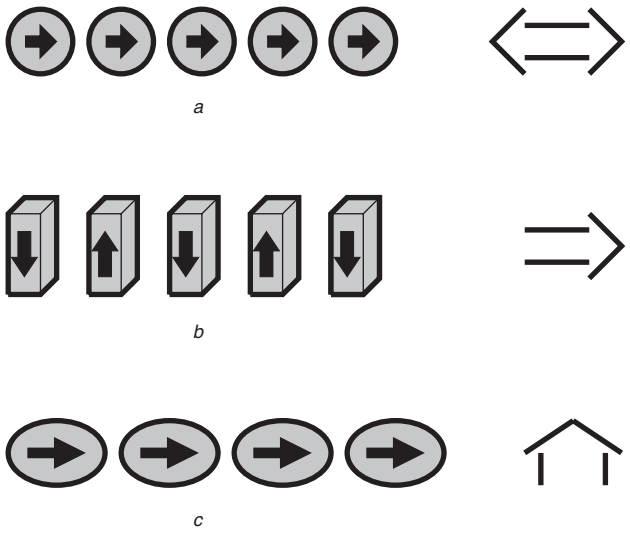

Fig. 1 *Three current MCA systems*
Each device is a single-domain nanomagnet with maximum dimensions of a few hundred nanometres. The arrow within each element illustrates the direction of its net magnetisation. The arrow on the right illustrates which direction the external clock field is applied
a Cowburn and Welland's MQCA [2]. Each nanomagnet is a circular disk 10 nm thick, with a diameter of 110 nm
b Csaba et al.'s magnetic logic [3]. Each nanomagnet is parallelopiped with dimensions of perhhaps $20 \times 20 \times 100$ nm
c Parish and Forshaw's BMQCA [4, 5]. Each element is a planar ellipse approximately 10 nm thick with a major/minor axis of 150/100 nm

One significant difference between the MQCA and an EQCA system is the method of clocking. As described above, in the MQCA system signals were forced along the wire using an external magnetic driving field. However, signal propagation occurs in EQCA systems via adiabatic clocking. In EQCA systems, the solution to a problem is mapped directly to the ground state of the system. The active elements are raised into a high energy (or null) state by an external clock field. Inputs are then applied at the edge of the array. These define the ground state into which the system evolves, as the clock field is reduced. To ensure that the system evolves towards its ground state and not

IEE Proceedings online no. 20040746
doi:10.1049/ip-cds:20040746
Paper first received 13th October 2003 and in revised form 8th April 2004. Originally published online: 26th October 2004

The authors are with the Department of Physics and Astronomy, University College London, London WCIE 6BT, UK

towards a local (incorrect) energy minimum, the modulation of the clock field needs to occur at a rate which is slow compared to the rate at which the system reaches its equilibrium state (adiabatic evolution).

Two further MCA systems which do use adiabatic clocking have been proposed. Csaba *et al.*'s system is illustrated in Fig. 1*b* [3]. A second system, illustrated in Fig. 1*c*, was proposed by Parish and Forshaw [4, 5]. In both of these systems, bistability is achieved (even in isolated elements) by using elongated nanomagnets. It is thought that this increases system performance and ensures that arbitrary circuit designs can be implemented.

Csaba *et al.*'s system is based on using parallelopiped nanomagnets, which form an array of pillars. In an analogous manner to EQCA systems, computation is conducted by applying input signals at the edge of the array. An external magnetic field is then used to reorientate (or clock) the moments of the elements so that they point parallel to their hard axes (the direction illustrated by the arrow at the right of the chain in Fig. 1*b*). As the magnetic field is reduced the moments relax into their ground state configuration. In this system the ground state is antiferromagnetic: adjacent moments point in opposite directions. Results based on SPICE modelling suggested that clocking speeds of up about 100 MHz should be possible with such systems.

The bistable magnetic quantum cellular automata (BMQCA) system proposed in [4, 5] is similar to the two systems described above. Planar nanomagnets are used as in [2]; however, like the system in [3], adiabatic evolution is used to clock the elements. Bistability is introduced by using planar elliptical nanomagnets, with in-plane dimensions of perhaps 150 nm by 100 nm and 10 nm thickness. The elliptical profile ensures that the rotation of the moments under interelement interactions and coupling to the clocking field is as smooth and reproducible as possible; this maximises the frequency at which the system can reliably operate. Note that the sharp corners associated with the angular shape of the elements in [3] may give rise to strong demagnetising fields, unstable evolution and a four-fold symmetric ground state. Adiabatic evolution of the BMQCA system occurs using a modulating clock field parallel to the hard axis of the elements (as illustrated in Fig. 1*c*.

We have developed a micromagnetic simulator which incorporates finite temperature and realistic factors such as fabrication errors and other defects. This has been used to investigate the behaviour of both individual BMQCA elements and arrays of elements. It is shown that for successful adiabatic evolution of real MCA systems (at finite temperature and including defects) clocking must occur at a much slower rate than simple theory suggests.

2 Micromagnetic simulator

In view of Aharoni's criticisms of many micromagnetic simulators [11], and the wide variety of solutions which have been presented for the μMAG 'standard' problems [12, 13], we have developed a model [4], which when used under the appropriate conditions, can accurately reproduce room temperature, experimental results. The core of the program is based on a Monte Carlo (MC) model, which uses Metropolis updating to simulate thermal effects; it is also possible to use the program for gradient descent (GD) simulations. In micromagnetics, simulations based on the Landau–Lifshitz–Gilbert (LLG) equation are often used instead of MC, because they describe the true dynamic evolution of the system. However, the time step required for LLG simulations has to be smaller than the spin precession time ($\approx 10^{-10}$ s). Simulations are therefore currently limited to submillisecond time periods. To assess the long term stability of a system, longer time periods need to be accessed. The switching of elements using fields applied along the easy axis involves significant problems of time dependent phenomena associated with the attempt frequency for passage over the anisotropy energy barrier. We therefore initially avoided the need for real time quantification by investigating only the effects of external fields that are applied along the hard axis, which does not involve time dependence. We have carried out a large number of simulations on single elements, in which each simulated spin in the model represents a volume of magnetic material with all dimensions $< l_{ex}$nm, where $< l_{ex}$ is the exchange length (for supermalloy $< l_{ex} \approx 5$ nm).

Figure 2 presents experimental, theoretical and simulated hard axis saturation fields for 2:1 (major-to-minor axis aspect ratio), planar supermalloy ellipses with a thickness of 5 nm and a simulated temperature of 300 *K*; the theoretical and experimental data are taken from [14]. The experimental values are generally a factor of two smaller than both the theoretical results and the gradient descent results. In [14] it is argued that imperfect lateral profiles (due to fabrication errors) give rise to a surface anisotropy energy which opposes the conventional shape anisotropy. However, our simulated results give good agreement with experiment without any significant edge roughness (only the inherent discretisation roughness was present). Including a simulated edge roughness decreased the accuracy of the MC results: in general the simulated saturation field increased, by as much as 30% in small elements.

At simulated room temperature, the magnitude of an element's moment $m \approx (0.7\text{–}0.8) M_S V$, where M_S is the saturation magnetisation and V is the volume of the element. Thus, although there is good agreement between experiment and the simulation results, it is not completely clear whether this is a simulation artifact or a real phenomenon. It may be because micromagnetic simulators treat systems classically: the well-known shape of the Curie–Weiss curve is best described using quantum theory [15]. It is nevertheless evident that temperature-dependent processes cannot be ignored in micromagnetic simulators.

When trying to analyse the behaviour of groups of elements, explicit calculation of the magnetostatic interactions can be computationally expensive. To allow arrays of interacting elements to be simulated in an acceptable time

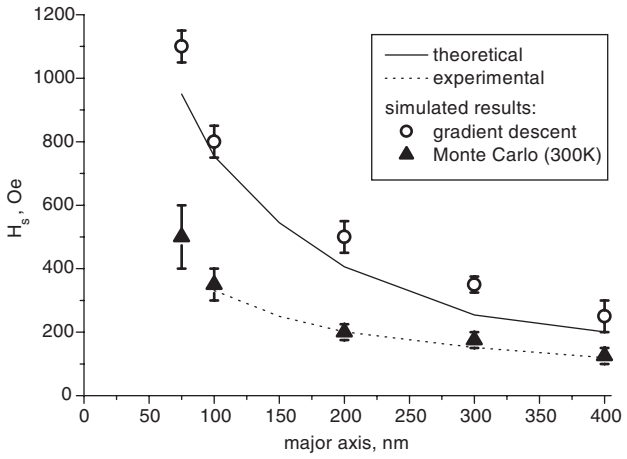

Fig. 2 *Hard axis saturation field for 2:1 aspect ration ellipses of 5 nm thick supermalloy*
The theoretical data and experimental results are taken from [11]

period, the spatial resolution of the simulator was reduced. At this lower resolution each simulated spin represents the macrospin of an entire nanomagnet (for example, a planar ellipse with dimensions $150 \times 75 \times 5$ nm, which is a volume of approximately 50 000 nm^3). Figure 3 plots high-resolution results and two sets of low-resolutions results for a 5 nm 2:1 supermalloy ellipse with a major axis of 150 nm. Much closer agreement with the high-resolution data is achieved if the magnitude of the moment is reduced from the theoretical value of $M_S V$ and is allowed to vary temporally by ± 0.05 $M_S V$ to simulate thermal fluctuations. The experimental value for the saturation field for such an element is approximately 250 Oe, although it has been shown that the magnitude of this field is very sensitive to small changes in dimension [16].

MC time quantification has been included in the low-resolution simulator by using the method suggested by Nowak *et al.* [17, 18]. They showed that for an isolated spin, or for one in a line of spins, the characteristic escape time for thermal activation over an energy barrier could be related to $1/R^2$, where a random Monte Carlo spin kick vector, sampled from a uniform distribution over a sphere or radius R, is added to the spin, which is then renormalised. They could then derive an expression for the relationship between R and a 'real' time interval Δt:

$$R^2 = 20\alpha\gamma kT\Delta t/((1+\alpha^2)\mu_s)$$

where $\alpha =$ damping factor; $\gamma =$ gyromagnetic ratio; and $\mu_s =$ spin moment, k is Boltzmann's constant and T is the absolute temperature. They showed that, in the high damping regime ($\alpha \geq 1$), the predictions of their model agreed very well with those of the Landau–Lifshitz–Gilbert theory: see [17, 18] for details. In the present work α was set equal to 2. The accuracy of the low resolution model at simulating time-dependent phenomena was tested by simulating the MQCA system presented in [2]. Figure 4 plots the magnetisation of the MQCA wire (measured within the plane of the system) as a function of time. Realistic parameters have been included: for example, a value of $m = 0.72 M_S V$ with a temporal variation of 0.1 $M_S V$ was used for the moment of each 110 nm supermalloy disc; this value was estimated from high-resolution simulations of a single element. The simulations also incorporated

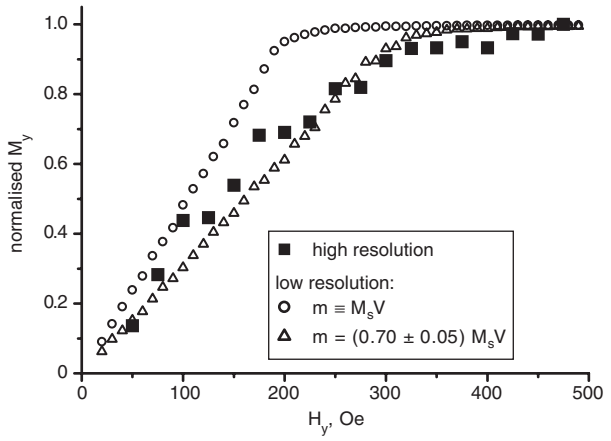

Fig. 3 *Hard axis behaviour of a 5 nm thick element with $a = 150$ nm and $AR = 2$*
The experimental value for this element is ≈250 Oe. The high resolution, simulated result is ≈300 Oe. The more accurate result achieved with the lower resolution model was obtained when the moment of the element was reduced and allowed to fluctuate over time (to simulate the effects of thermal fluctuations)

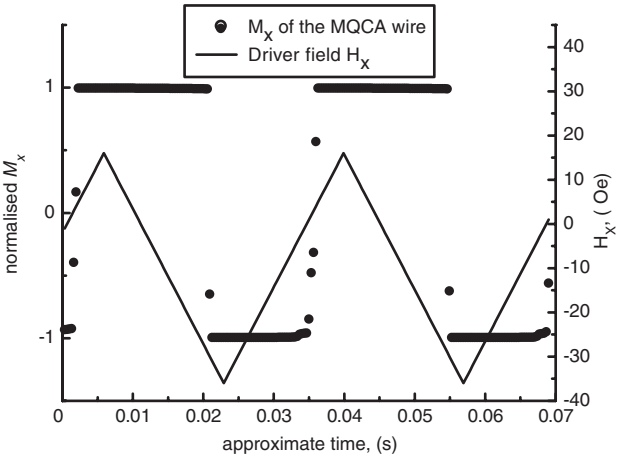

Fig. 4 *Simulated behaviour of a chain of 69 MQCA elements*
The dots illustrate the magnetisation parallel to the wire axis at each external field value. The continuous line represents the variation in the external driver field

simulated fabrication errors such as slight misalignment of the elements along the wire, and a small degree of shape anisotropy due to a non-circular profile. In the experimental system [2], a square wave driving field was used and the resolution of the equipment was insufficient to accurately measure the switching fields of the wire. The magnitudes of the two switching events were approximately equal to (but not greater than) |10| Oe and |35| Oe. In the simulated system the two switching fields were $|4.6 \pm 0.7|$ Oe and $|30.4 \pm 1.8|$ Oe; using $m \equiv M_S V$; if the 'realistic' factors were left out then the values were approximately 10 Oe and 50 Oe.

One essential requirement for a BMQCA element is that it should be stable against temperature fluctuations. It may be shown that an anisotropy energy of about $60kT$, for $T = 300\,K$, is needed if large assemblies of elements, more than 10^9 in number, are not to exhibit frequent and undesirable spin flips in any of the elements. A range of stability results is presented in [4]: for example, it was found that for ellipticities between about 1.5:1 and 5:1, the anisotropy energy barrier was almost independent of the ellipticity and varied monotonically with the length, being about $60kT$ ($T = 300\,K$) for a 100 nm long, 5 nm thick supermalloy ellipse.

3 BMQCA

Once the accuracy of the micromagnetic model had been established, it was used to investigate the performance of a number of BMQCA systems. As briefly described in Section 1, a BMQCA system is an array of interacting planar elliptical nanomagnets. Figure 5 illustrates three wire geometries and a simple logic unit. By combining these and the ferromagnetic planar wire illustrated in Fig. 1*c*, it is possible to design arbitrary circuits. Like EQCA systems, MCA will probably be clocked in groups or common zones [7, 19]. Anti-ferromagnetic wires are, *ceteris paribus*, less stable than ferromagnetically coupled wires [4], but the propagation of solitons ('kinks') is otherwise broadly similar in both cases.

Representative data from two ten-element ferromagnetic, planar wire simulations using our low-resolution model are shown in Figs. 5 and 6. In each simulation the clock field was applied globally: it had a magnitude approximately twice the magnitude of the hard axis saturation field (for an individual element), and was parallel to the short axis of the

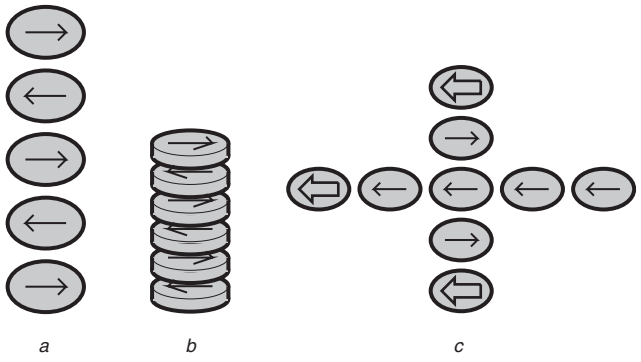

Fig. 5 *Three BMQCA subcircuit designs*
a Antiferromagnetic planar wire
b Antiferromagnetic vertical (or stacked) wire
c Majority gate

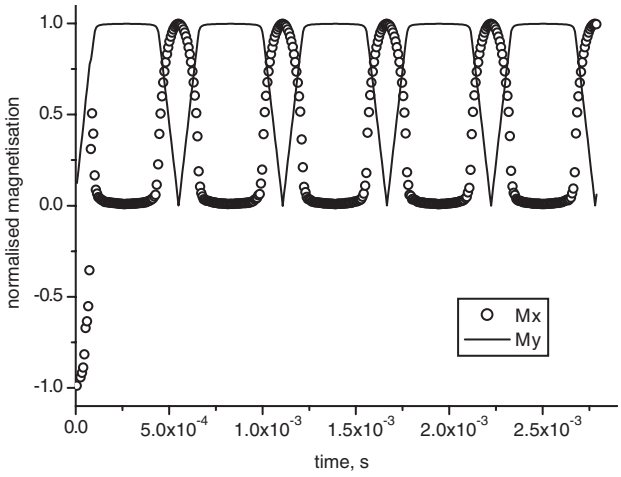

Fig. 6 *Simulated inplane magnetisation for a ten-element ferromagnetic planar wire*
Each element was a 5 nm thick supermalloy planar ellipse of aspect ratio 1.5:1 with a major axis of 150 nm. The clock field frequency was 1.8×10^3 Hz. This illustrates good switching reliability

ellipses (as illustrated in Fig. 1*c*). When the clock field is high (usually several hundred oersted) the moments of the elements should lie approximately parallel to their hard axes. As the field is slowly reduced the moments rotate towards their easy axes. The direction of the moments in their ground state should correspond to the direction of the input moment. The input signal was represented by a fixed magnet, which pointed in the positive x direction and was present throughout the simulations. Therefore, in Figs. 6 and 7, at zero field (not shown but easily estimated from the M_y component) the moments of the BMQCA should point in the $+x$ direction. We present the normalised magnetisation: at zero field, a successful switch of the whole line of elements is represented by $M_x \approx 1.0$ and $M_y \approx 0.0$. The initial orientation of the moments was -1; this is not included in the estimation of reliability.

Figure 6 represents the evolution of ten supermalloy elements, each with a long axis of 150 nm, an aspect ratio of 1.5 and a thickness of 10 nm. The pitch of the wire (centre-to-centre element separation) was 175 nm and the clock frequency was 1.8×10^3 Hz. Only the first five cycles of the 100 which were simulated are shown. The system switched correctly at each of the 100 attempts. Therefore, we give the system a reliability of 1.0 (simply defined as the number of successful switches divided by the number of attempts).

Figure 7 illustrates an unreliable system. In this simulation the supermalloy elements had a major axis of

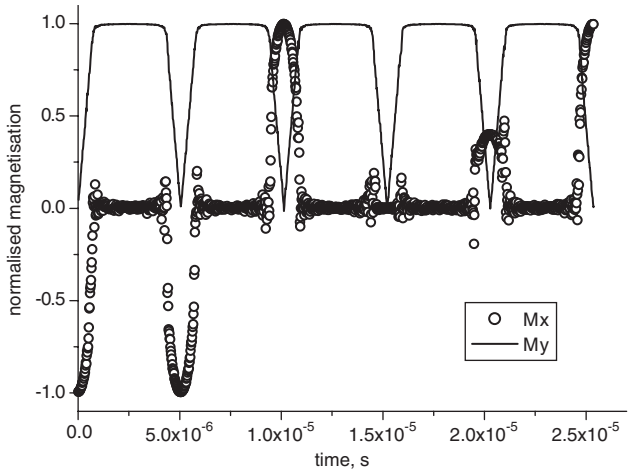

Fig. 7 *Simulated inplane magnetisation for a ten-element ferromagnetic planar wire*
Each element was a 5 nm thick supermalloy planar ellipse of aspect ratio 2.5:1 with a major axis of 100 nm. The clock field frequency was 2.0×10^5 Hz. This illustrates poor switching reliability

100 nm, an aspect ratio of 2.5 and a thickness of 5 nm. The pitch of the wire was 125 nm and the clock frequency was 2.0×10^5 Hz. It can be seen that of the five attempts, the wire switched correctly only twice: its reliability for 100 attempts was 0.36. The system did saturate along its hard axis (M_y saturates at 1.0) which shows that a sufficiently high clock field was used. However, as the clock field was reduced the system failed to find its global minimum. The clock field varied too rapidly for successful adiabatic evolution: thermally induced spin kicks produced solitons ('kinks'), separating regions of the wire with opposite spin alignment. The system frequently became trapped in a local energy minimum instead of evolving towards the ideal global energy minimum with all of the spins pointing in the same direction as the input element. For example, on the third attempt, $M_x \approx 0.0$, which means that half of the moments pointed in the correct direction but the other half of the moments pointed in the opposite direction. If solitons appeared then they could only be removed by thermal fluctuations of sufficient size (in combination with the residual long-range influence of the input) to drive them off the end of the wire. If the clock frequency is too high, then thermal fluctuations do not have sufficient time to drive the system out of the local minima.

We have investigated a number of BMQCA system parameters, including: element dimensions (major axis, thickness and aspect ratio), wire pitch, material, temperature, system size and the effect of fabrication defects (for example variation in position and variation in anisotropy energy).

Figure 8 illustrates two important points. First, as the clock frequency increases, the system progressively departs from true adiabatic evolution and the reliability is reduced. Second, the reliability is also reduced when realistic factors are included, such as misalignment of the elements along the wire, variation in the magnitude of each moment, and a small variation in shape anisotropy amongst the elements. These factors, although significant, are of lesser importance than the inclusion of temperature dependence. It is also essential to model the interaction terms between all of the elements, and not just nearest-neighbour interactions.

Ideally one would like to maximise the interaction between neighbouring elements, so that signals can be propagated rapidly down a wire for example. However, it is also necessary for the elements to be physically separate

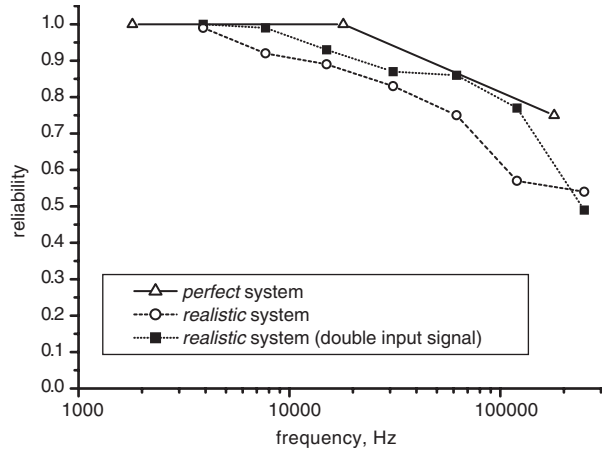

Fig. 8 *Simulated reliability of a 10-element ferromagnetic wire*
Each supermalloy element had an easy axis of 150 nm, an aspect ratio of 1.5 and was 5 nm thick; the pitch of the wire was 175 nm. 'Realistic' means that $\bar{m} = (0.72 \pm 0.05)M_S V$, there was a ± 2 nm error in dot positions and there was also a 3% variation in the shape anisotropy amongt the elements. It can be seen that as clock frequency is increased and when realistic factors are included, the reliability decreases

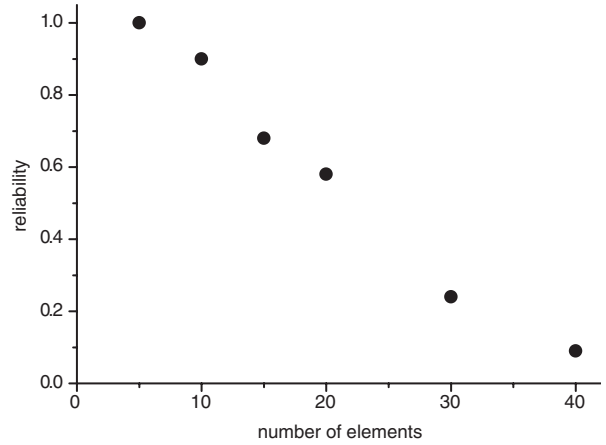

Fig. 9 *Reliability of a ferromagnetic, planar wire with respect to the number of BMQCA elements it contains*
Each element had a long axis of 150 nm, an aspect ratio of 1.5 and the pitch of the wire was 175 nm. The simulated temperature was 300 K. For each simulation the clock field frequency was approximately 2 kHz. As the number of elements in the system increases, so the reliability decreases

(they must not touch one another), and they must be individually bistable in the presence of external perturbing fields and thermal fluctuations. If the individual elements are too large (more than a few hundred nanometers long for supermalloy) then domain walls appear, and the individual elements no longer exhibit spin coherence. Further work is in progress to see how small the elements can be made while retaining sufficient stability.

Figure 9 illustrates the variation in the reliability of a wire with respect to the number of elements which are coherently clocked. Each element had a long axis of 150 nm and an aspect ratio of 1.5, and the interelement pitch was 175 nm. For each simulation the clock field frequency was approximately 2 kHz. Each additional element further complicates the energy surface that the system has to negotiate. If the clock frequency is too high, and if evolution is not occurring adiabatically, then the system is unlikely to

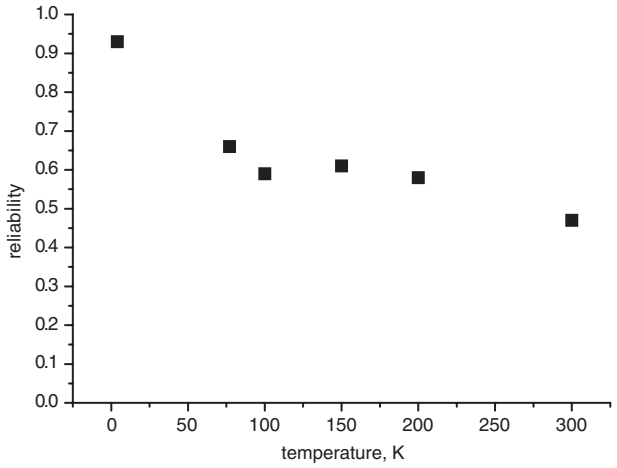

Fig. 10 *Reliability as a function of temperature of a ferromagnetically coupled wire consisting of ten active elements, with $a = 150$ nm, $AR = 1.5$, and thickness 5 nm*
Each system was operating at approximately 0.5 MHz

find its true global ground state and is more likely to settle into an incorrect local minimum.

Figure 10 shows that reliability varies with operating temperature. Systems are more reliable at low temperatures, where thermally induced spin fluctuations do not perturb the system from the ideal path that links the high-energy starting state to the low-energy final state. The relationship between reliability and temperature does not appear to be linear.

4 Implications for MCA Systems

Our results raise a number of important issues. They imply that, to ensure the successful adiabatic evolution of a group of MCA elements at room temperature, the maximum frequency of operation is likely to be significantly lower than that calculated for the same system at zero kelvin. The main reason for this is that, at the start of each clock cycle, the system is in an energy state such that thermally induced spin fluctuations can easily move it into an undesirable metastable energy state, which can only be exited by waiting for another thermal fluctuation to kick the system back on to the correct track. At 0 *K*, both single elements and groups of elements can in principle switch very quickly, perhaps at hundreds of megahertz, being limited mainly by spin precession effects. At or near 300 *K*, it seems probable that the maximum operating speeds may be over 1000 times slower than this ideal maximum, even if non-uniformity of the element sizes, shapes and positions is discounted.

There are also other problems associated with adiabatic magnetic logic systems. If an external magnetic field, generated by a single wire, is used to execute clocking, then the system is likely to require an unacceptable amount of power. Generating the required field, at a distance of a few tens of nanometers under the wire, requires a current of the order of a few milliamps. However, the small wire cross-section (for example, 1 μm × 1 μm), and the need for global clocking means that the power dissipation would be 100–1000 W cm^{-2}. Indeed, a value of approximately 1 kW cm^{-2} has been published for an experimental system with similar attributes [20]. Most MRAM systems use a grid of wires, but they do not encounter power dissipation problems because their elements require smaller fields, and are switched individually from one state to another, rather than being adiabatically clocked in parallel. Some possible

ways to clock blocks of BMQCA elements are outlined in [4], but it must be emphasised that it is likely to be difficult to devise a realistic method. One may note for comparison that, to the best of the authors' knowledge, no practical clocking scheme has been described for electronic QCA systems in a decade of research.

5 Conclusions

In this paper we have attempted to address some of the issues relating to complete MCA systems, which have not been previously examined. We began by introducing the three main MCA systems. The MC/Metropolis magnetic model was then explained, and subsequently used to investigate a range of factors connected to the BMQCA device. A selection of results was presented, the most significant perhaps being the demonstration of the deleterious effects of temperature and system size on the maximum clock frequency at which groups of BMQCA devices can be operated reliably, when compared to the maximum frequency of a single element at $0\,K$. Similar behaviour was observed when realistic variations in device size, shape and position were simulated. These are factors which are rarely addressed in the current literature. We suggest the problems associated with adiabatic evolution of magnetic quantum cellular automata at finite temperatures may also apply to EQCA and to some quantum adiabatic systems.

6 Acknowledgment

The authors thank the referees for their helpful comments. M. Parish was supported by a UK EPSRC studentship.

7 References

1 Waser, R. (ed.): 'Nanoelectronics and information technology' (Wiley-VCH, 2003), Chap 4, 23 and 24
2 Cowburn, R., and Welland, M.: 'Room temperature magnetic quantum cellular automata', *Science*, 2000, **287**, pp. 1466–1468
3 Csaba, G., Imre, A., Bernstein, G.H., Porod, W., and Metloshki, V.: 'Nanocomputing by field-coupled nanomagnets', *IEEE Trans. Nanotechnol.*, 2002, **1**, pp. 209–213
4 Parish, M.: 'Modelling of physical constraints on bistable magnetic quantum cellular automata'. PhD Thesis, University of London, July 2003, See http://ipga.phys.ucl.ac.uk/
5 Parish, M., and Forshaw, M.: 'Physical constraints on magnetic quantum cellular automata', *Appl. Phys Lett*, 2003, **83**, pp. 2046–2048
6 Wolfram, S.: 'A new kind of science' (Wolfram Media, 2002)
7 Lent, C., and Tougaw, D.: 'A device architecture for computing with quantum dots', *Proc. IEEE*, 1997, **85**, pp. 541–557
8 Cowburn, R.P., Koltsov, D.K., Adeyeye, A.O., Welland, M.E., and Tricker, D.M.: 'Single-Domain Circular Nanomagnets', *Phys. Rev. Lett.*, 1999, **83**, pp. 1042–1045
9 Orlov, A.O., Ainlani, I., Totn, G., Lent, C.S., Bernstein, G.H., and Snider, G.L.: 'Experimental demonstration of a binary wire for quantum-dot cellular automata', *Appl. Phys. Lett.*, 1999, **74**, pp. 2875–2877
10 Amlani, I., Orlov, A.O., Snide, G.L., Lent, C.S., and Berstein, G.H.: 'Demonstration of a six-dot quantum cellular automata system', *Appl. Phys. Lett.*, 1998, **72**, pp. 2179–2181
11 Aharoni, A.: 'Micromagnetics: past, present and future', *Physica B*, 2001, **306**, pp. 1–9
12 http://www.ctcms.nist.gov/rdm/toc.html
13 Donahue, M., Porter, D., and McMichael, R.: 'Behavior of μMAG standard problem No.2 in the small particle limit', *J. Appl. Phys.*, 2000, **87**, pp. 5520–5522
14 Cowburn, R.P., Koltov, D.K., Adeyeye, A.A, and Welland, M.E.: 'Lateral interface anisotropy in nanomagnets', *J. Appl. Phys.*, 2000, **87**, pp. 7067–7069
15 Chikazumi, S.: 'Physics of ferromagnetism, No.94 in International Series of Monographs on Physics' (Oxford Science, 1997)
16 Cowburn, R.: 'Superparamagnetism and the future of magnetic random access memory', *J. Appl. Phys.*, 2003, **93**, pp. 9310–9315
17 Nowak, U., Chantrell, R., and Kennedy, E.: 'Monte Carlo simulation with time step quantification in terms of langevin dynamics', *Phys. Rev. Lett.*, 2000, **84**, pp. 163–166
18 Hinzke, D., and Nowak, U.: 'Magnetic relaxation in a classical spin chain', *Phys. Rev.*, 2000, **B61**, pp. 6734–6740
19 Berzon, D., and Fountain, T.: 'A memory design in QCAs using the SQUARES formalism'. Proceedings of the Ninth Great Lakes Symposium on VLSI, 1999, pp. 166–169
20 Drndić, M., Johnson, K.S., Thywisses, J.H., Prentiss, M., and Westervekt, R.M.: 'Micro-electromagnets for atom manipulation', *Appl. Phys. Lett.*, 1998, **72**, pp. 2906–2908